

Supporting information

Porous diamond carbon framework: A new carbon allotrope with extremely high gas adsorption and mechanical properties

Ling Huang, Zhonghua Xiang and Dapeng Cao*

State Key Lab of Organic-Inorganic Composites, Beijing University of Chemical Technology, Beijing 100029, China. *E-mail: caodp@mail.buct.edu.cn

This supporting information provides (1) a D-carbon.cif file (2) Relative energy calculation; (3) Details for GCMC simulation; (4) Details for calculation of mechanical property; (5) Calculation for the isosteric heat; (6) Calculation for the Band structure.

S1. Relative energy calculations

In order to explore the relative energies between D-carbon and some isomeric carbon structures, by using the calculation approach mentioned in literature,^{1,2} one can define a molar Gibbs free energy (δG) of material formation as $\delta G(\chi_i) = E(\chi_i) - \sum_i \chi_i \mu_i$, here $E(\chi_i)$ is the cohesive energies per atom of D-carbon, CNT(5,5) and diamond respectively with given composition and dimensions. χ_i is the molar fraction of the carbon in the systems, and μ_i is the chemical potential of the constituent i at a given state. We used the cohesive energy per atom of the single infinite graphene to represent μ_C . The calculated results were listed in Table S1. The calculated cohesive energy and formation energy for CNT(5,5) are

-7.843 eV/atom and 0.1506 eV/atom respectively, both of which are in agreement with the results previously reported by Barone *et al.*³ and Zhang *et al.*,¹ indicating the accuracy of our method. By comparison with CNT and diamond, it is found that D-carbon is also energetically favored and thermodynamically stable, because the formation energy of D-carbon is larger than those of CNT and diamond significantly.

Table S1. The calculated cohesive energy and formation energy for CNT(5,5), diamond and D-carbon.

Structures	Cohesive energy (eV/atom)	Formation energy (eV/atom)
CNT (5,5)	-7.8707	0.1506
diamond	-7.9105	0.1108
D-carbon	-6.8721	1.1493

S2. Details for GCMC simulation

During the GCMC simulation, periodic boundary conditions were imposed in all directions and the LJ potentials were cutoff at the position of the half of the minimal box size. For each pressure point, 3×10^7 configurations were generated, where the first 1.5×10^7 configurations were discarded to guarantee equilibration and the second 1.5×10^7 configurations were divided into 10 blocks to calculate the ensemble average. The uncertainties on the final results, including the ensemble averages of the number of adsorbate molecules in the simulation cell and the total potential energy, were estimated to be within $\pm 2\%$.

As well known, to accurately describe the CH₄ adsorption behavior in an all-carbon skeleton D-carbon framework, choosing a set of appropriate potential parameter for

carbon atom is a prerequisite. To our knowledge, sp^2 -hybridized carbon atom described by UFF and Dreiding force fields was frequently adopted to investigate adsorption properties of COFs^{4,5} and IRMOFs.⁶ In addition, carbon model from graphite is often chosen to represent the interaction of sp^2 - sp^2 hybridized carbon atoms within ordered carbon adsorbent CMK-1⁷ and fullerene intercalated graphite.⁸ However, the sp^3 -hybridized carbon atom was mainly described by UFF and Dreiding force fields. Actually, a different force field was also used to represent the sp^3 -hybridized-C group model of neopentane.⁹

Since the D-carbon is a new material, no any experimental data is available for confirming its adsorption property. Accordingly, regarding the analogy of D-carbon and COFs in the hybridized state of carbon atoms, we intend to adopt experimental data of methane adsorbed in COF-102 as a calibration to screen out a proper potential parameter to represent the D-carbon. We first used UFF and Dreiding force fields to calculate the methane uptake of COF-102. It was found that both force fields lead to a significant overestimation of methane adsorption, although Dreiding force field is better than UFF force field, compared to the experimental methane uptake,¹⁰ as shown in Figure S1. Actually, the same overestimation of 20% for CH_4 uptake was also reported by Garberoglio,¹¹ where they adopted the Dreiding and UFF force fields.

To improve the calculation accuracy, we also adopted two different types of carbon atom parameters to recalculate methane uptake of COF-102. In this calculation, we used the carbon parameter of graphite to describe sp^2 -C, and the sp^3 -hybridized carbon of neopentane to represent sp^3 -C, while the other elements (B, H, O) in COF-102 were described by Dreiding force field. The adopted parameters were listed in Table S2, and the

corresponding calculation result of methane adsorption in COF-102 at 298 K was also presented in Figure S1. Surprisingly, the recalculation result excellently reproduces experimental methane isotherm of COF-102, which validated the reliability of the selected two different types of carbon atom parameters. Therefore, in the following calculation of CH₄ adsorption in D-carbon, we adopted the screened two-type-carbon potential model to represent the sp²-hybridized and sp³-hybridized carbon atoms, respectively, which was summarized in Table S3.

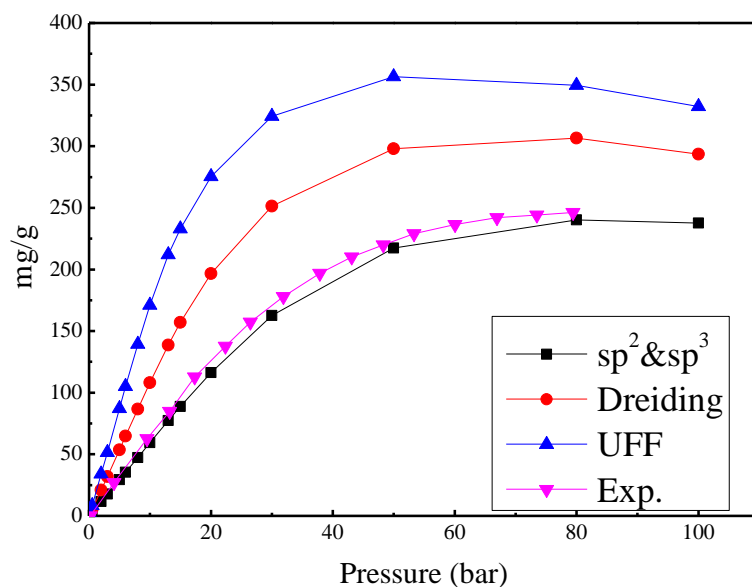


Figure S1. High-pressure CH₄ isotherms in COF-102 using UFF, Dreiding and two-type-carbon potential models, respectively, at 298 K.

Table S2. LJ potential parameter for CH₄ adsorption in COF-102.

Elements	LJ parameters	σ (Å)	ε/k_B (K)	Ref.
sp ² -C		3.4	28.0	7,8,12
sp ³ -C		3.8	25.16	9
H		2.85	7.65	13
B		3.58	47.8	13
O		3.03	48.16	13
CH ₄		3.73	148.0	14,15
He		2.58	10.22	15,16

Table S3. LJ potential parameter for CH₄ adsorption in D-carbon.

Elements	LJ parameters	σ (Å)	ε/k_B (K)	Ref.
sp-C		3.4	28.0	7,8,12
sp ³ -C		3.8	25.16	9
CH ₄		3.73	148.0	14,15
He		2.58	10.22	15,16

S3. Details for calculation of mechanical properties

The bulk modulus is calculated by VASP with LDA, using the Voigt-Reuss-Hill approximation.¹⁷ We can obtain the bulk modulus derived by the $\frac{\Delta E}{V} \sim \delta$ relationship, given by

$$\frac{\Delta E}{V} = \frac{9}{2} \times B \delta^2 \quad (\text{S1})$$

where B is the bulk modulus, and δ is varying from -0.02 to 0.02 in steps of 0.002. The 21 sets of $\frac{\Delta E}{V} \sim \delta$ data were then fitted by using a quadratic polynomial equation and B (eV/Å³) was obtained by the coefficient of the quadratic term. Using the method, the bulk modulus of diamond was calculated by fitting into a quadratic polynomial equation given in Figure S2. By converting the unit (eV/Å³) of B into GPa, we can obtain the calculated

bulk modulus of diamond and it is 474.83 GPa, which is comparable with its experimental value of 443 GPa.¹⁸ Hence, in this work, we believed that the bulk modulus of D-carbon calculated by the same method above is reliable.

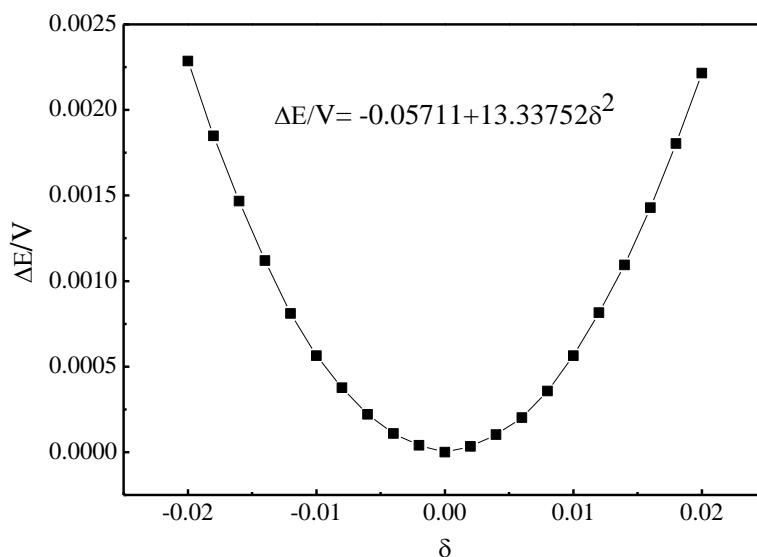


Figure S2. The bulk modulus calculation of diamond.

Table S4. The calculated elastic constants for diamond and D-carbon

Elastic constants (GPa)	C_{11}	C_{12}	C_{44}
diamond	1114.08	155.183	598.363
D-carbon	98.288	88.36	14.132

After the independent elastic constants (C_{11} , C_{12} and C_{44}) describing single crystal properties were obtained by the above procedure and listed in Table S4, the elastic moduli (e.g., the shear modulus) can be also estimated by the Voigt-Reuss-Hill approximation.¹⁷

In the approximation, the shear modulus of a material is given by

$$G = \frac{1}{2}(G_V + G_R) \quad (S2)$$

where, G_V is the shear modulus of cubic lattice from the Voigt average, and G_R is the

shear modulus from the Reuss average, given by

$$G_V = \frac{1}{5}[(c_{11} - c_{12}) + 3c_{44}] \quad (\text{S3})$$

$$G_R = \left[\frac{4}{5}(c_{11} - c_{12})^{-1} + \frac{3}{5}c_{44}^{-1} \right]^{-1} \quad (\text{S4})$$

After the shear modulus G (see eq.(S2)) and bulk modulus B (see eq. (S1)) were obtained, the Young's modulus can be calculated by

$$E = \frac{9BG}{3B + G} \quad (\text{S4})$$

We used eq.(S4) to calculate the Young's modulus of D-carbon and diamond. The calculated Young's modulus of diamond is 1186.59 GPa, which is very close to its experimental value of 1050 GPa.¹⁹ The observation confirms the reliability of our calculations again. Table S5 lists the calculated Young's modulus E , bulk modulus B and shear modulus G of D-carbon and diamond.

Table S5. The calculated bulk modulus, shear modulus and Young's modulus for diamond and D-carbon.

Structures	Bulk modulus B (GPa)	Shear modulus G (GPa)	Young's modulus E (GPa)
diamond	474.82	547.58	1186.59
D-carbon	91.67	18.59	52.23

To further confirm the mechanical stability of D-carbon, the phonon spectra DOS of D-carbon is also calculated. As shown in Fig S3, no imaginary phonon mode is found in the phonon DOS of D-carbon, implying the kinetic stability of D-carbon.

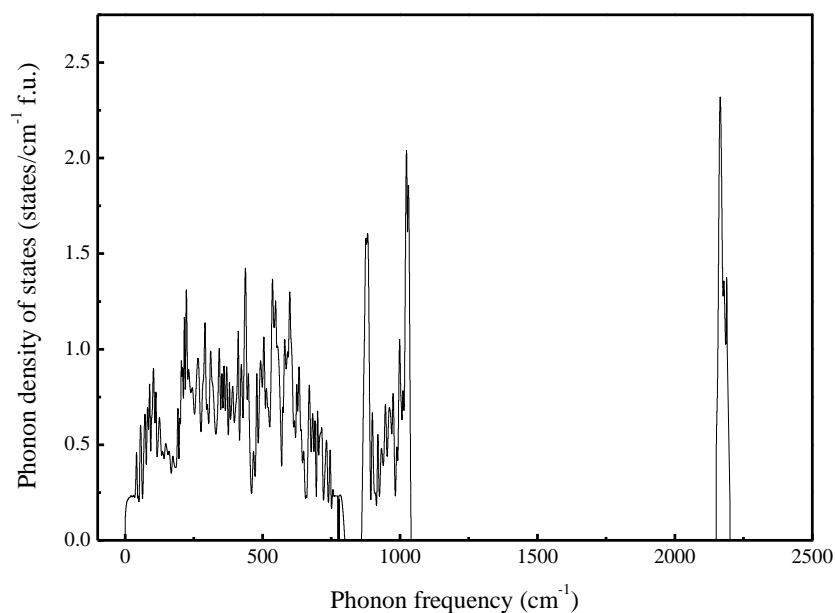


Figure S3. The phonon DOS of D-carbon.

S4. Calculation for the isosteric heat

Based on the fluctuation theory, the isosteric heat Q_{iso} , a thermodynamic quantity that reflects the heat released for each molecule added to the adsorbed phase, can be calculated.

²⁰ The isosteric heat of CH₄ in D-carbon was calculated and shown in Figure S4. It is 19.4 KJ/mol at the uptake of 0.01 mmol/g, which indicates that the adsorption is approximately within the range between the physisorption and chemisorption, indicating that methane stored in the host material could be released reversibly at room temperature without the need of higher temperatures.

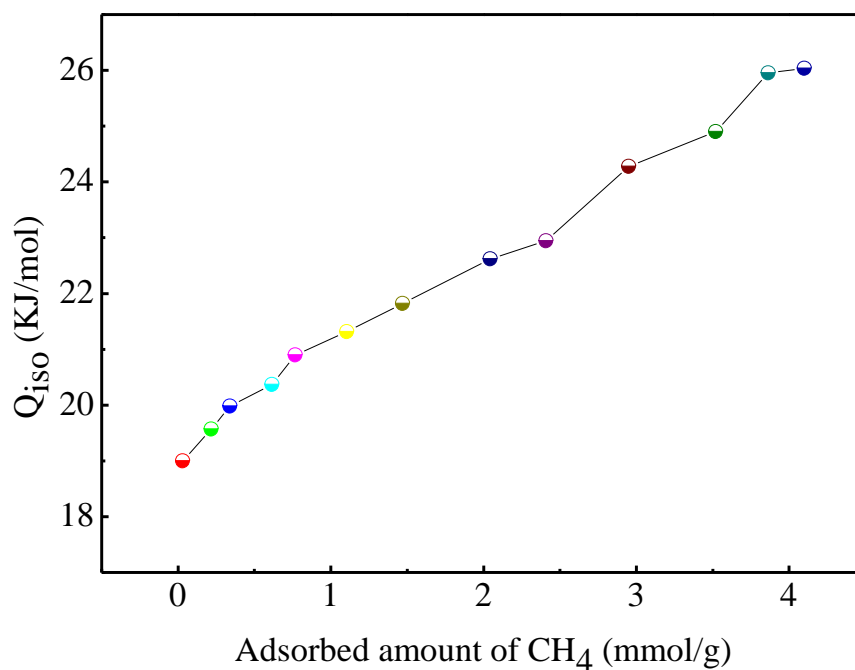


Figure S4. The calculated isosteric heat of CH₄ in D-carbon.

S5. Calculation for the Band structure

Band structures of CNTs, diamond, and D-carbon has been calculated. As shown in Figure S5, CNT(5,5) possesses conducting property while CNT(10, 0) shows semiconducting behavior, which is in agreement with the reported results in other literature. Actually, D-carbon shows a wide band gap of about 4.8 eV, so its electronic property is basically similar with diamond.

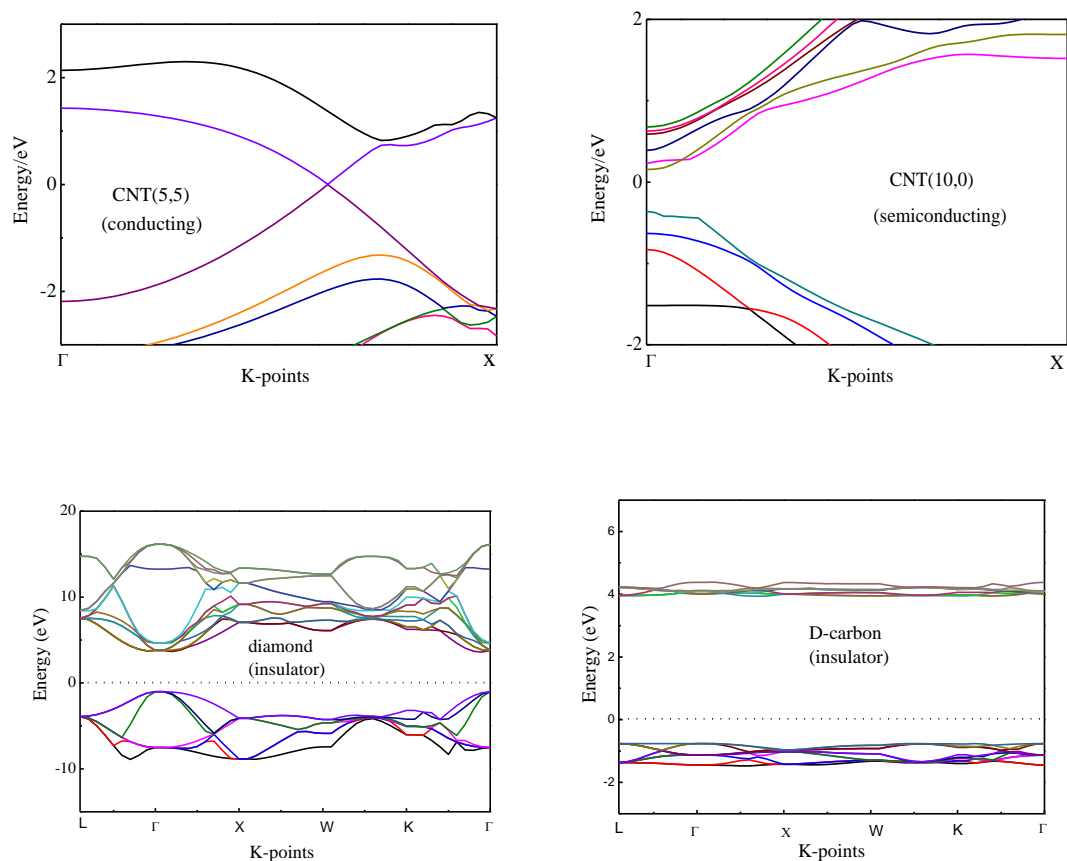


Figure S5 The calculated band structure of D-carbon. For comparison, the band structures of CNT(5,5), CNT(10,0) and diamond are also presented here.

References

1. Zhang, Z. Y.; Zhang, Z. H.; Guo, W. L. *J. Phys. Chem. C* **2009**, *113*, 13108-13114.
2. Barone, V.; Hod, O.; Scuseria, G. E. *Nano Lett.* **2006**, *6*, 2748-2754.
3. Hod, O.; Barone, V.; Peralta, J. E.; Scuseria, G. E. *Nano Lett.* **2007**, *7*, 2295-2299.
4. Yang, Q. Y.; Zhong, C. L. *Langmuir*, **2009**, *25*, 2302-8.
5. Mendoza-Cortes, J. L., Pascal, T. A., Goddard, III*, W. A. *J. Phys. Chem. A*, **2011**, *115*, 13852-7.
6. Jhon, Y. H., Cho, M., Jeon, H. R., Park, I., Chang, R., Rowsell, J. L. C., Kim, J. *J. Phys. Chem. C*, **2007**, *111*, 16618-25.
7. Peng, X., Cao, D. P., Wang, W. C. *J. Phys. Chem. C*, **2008**, *112*, 13024-36.
8. Peng, X., Cao, D. P., Wang, W. C. *Ind. Eng. Chem. Res.* **2010**, *49*, 8787-96.

9. Jorgensen, W. L.; Madura, J. D.; Swenson, C. J. *J. Am. Chem. Soc.* **1984**, *106*, 6638-46.
10. Furukawa, H.; Yaghi, O. M. *J. Am. Chem. Soc.* **2009**, *131*, 8875-83.
11. Garberoglio, G. *Langmuir* **2007**, *23*, 12154-8.
12. Do, D. D.; Do, H. D.; Kaneko, K. *Langmuir* **2004**, *20*, 7623-29.
13. Mayo, S. L.; Olafson, B. D.; Goddard, W. A. *J. Phys. Chem.* **1990**, *94*, 8897-909.
14. Martin, M. G.; Siepmann, J. I. *J. Phys. Chem. B* **1998**, *102*, 2569-77.
15. Peng, X.; Cheng, X.; Cao, D. *J. Mater. Chem.* **2011**, *21*, 11259-70.
16. Duren, T.; Sarkisov, L.; Yaghi, O. M.; Snurr, R. Q. *Langmuir* **2004**, *20*, 2683-89.
17. Hill, R. *Proc. Phys. Soc. A* **1952**, *65*, 349-354.
18. Andrievski, R. A., *Int. J. Refract. Met. Hard Mater.* , **2001**, *19*, 447-452.
19. Weidner, D. J., Wang, Y. B., Vaughan, M. T. *Science* **1994**, *266*, 419-22.
20. Lan, J. H.; Cao, D. P.; Wang, W. W., *Langmuir* **2010**, *26*, (1), 220-6.